International Journal of Innovative Technology and Exploring Engineering (IJITEE)
ISSN: 2278-3075 (Online), Volume-10 Issue-9, July 2021

Analysis and Design of Controller for Doubly-Fed Induction Generator in Wind Energy Application

Syed Sarfaraz Nawaz, S. Tara Kalyani

Abstract: ***Now a days, wind energy is developing as a significant wellspring of unpolluted and eco-friendly energy to supplant the enormous scope utilization of expendable wellsprings of energy. Wind Energy is pulling in enthusiasm of analysts everywhere throughout the globe as one of the most significant inexhaustible wellspring of energy. Be that as it may, the primary confinements lie in factor speed wind vitality. The under and above Synchronous speeds are obtained by utilizing a bidirectional power flow converter. In this paper a systematic transfer function model of a Doubly Fed Induction Generator based wind turbine structure connected to grid is developed in Mat lab/Simulink environment. The control structure of generator and that of turbine is developed and implemented. A simple approach is proposed to obtain the gains of Proportional Integral (PI) controller. A systematic detail of this control structure is presented. Under varying load conditions, it is observed that the reactive power is controlled and power factor of the system is maintained close to unity by using this scheme. Stator flux situated vector control method is conveyed for both stator and rotor side converters to supply autonomous control of active and reactive power and keep the DC link voltage consistent.***

Keywords: DFIG, PI controller, Rotating coordinate system, state space analysis, Stator Flux Oriented control.

I. INTRODUCTION

Wind is developing as a potential and a significant wellspring of sustainable power source on account of its enormous scope accessibility in a few regions and in sight of the points of interest concerning economy of intensity age with wind on a large scale[1]. The usage of wind plants is developing exponentially from the ongoing past. At first, the ordinary turbine was typically a simple induction generator which may apparently trip during unsettling influences, In fact, the wind plant did exclude the auxiliary administrations and upkeep of intensity quality. Yet, with the expanded infiltration of wind vitality transformation framework, the ongoing age of wind turbines has far more noteworthy capability [2]. The subordinate administrations necessities of the interconnected framework are frequently outfitted by the breeze park concentrated control frameworks.

Manuscript received on June 26, 2021.
Revised Manuscript received on July 01, 2021.
Manuscript published on July 30, 2021.
* Correspondence Author
S. Sarfaraz Nawaz*, Department of Electrical and Electronics Engineering, GRIET (JNTUH), Hyderabad (Telangana), India. Email: sarfaraz86nawaz@gmail.com
Dr. S. Tara Kalyani, Department of Electrical and Electronics Engineering, GRIET (JNTUH), Hyderabad (Telangana), India. Email: tarasunder98@jntuh.ac.in.

Besides, it helps the breeze plants to carry on simply like the conventional creating plants upheld synchronous machine at the hour of deficiency besides having dynamic reaction and control capacity. Because of whimsical and changing example of wind, one among the primary specialized concern is that the receptive force guideline inside the enormous breeze park. Additionally, to supply the necessary voltage backing to the network, receptive force pay is mandatory [3].

With the adjustment in power at various wind speeds, the measure of reactive power changes. [4] Meanwhile, with the developing size and subsequently the expanded number of wind plants which add to vitality creations, the responsive force delivered in huge scope Wind Park can't be disregarded. The impact of wind age on the vitality quality beard by power lattice may become uneconomic and even unreasonably expensive with the development of wind age scale [5]. Thusly, suitable breeze age pay inside wind age plant gets indispensable.

Mechanical drive applications are commonly grouped into steady speed and variable speed tasks. For variable speed applications dc machines are used where with respect to steady speed applications air conditioning machines are utilized for the most of the part [6]. In any case, on account of the inconveniences of dc machines lies for the majority section with brushes and commutators which limit the speed of the machine and its peak current. Accordingly air conditioning machines are rising more significantly than the dc machines as of late for variable speed applications. in order to fulfill power needs, contemplating affordable and natural components, wind vitality change is progressively picking up enthusiasm as a proper wellspring of inexhaustible energy [7]. With expanded penetration of wind age into electrical frameworks, wind turbines are generally sent gratitude to their variable speed and thus affecting framework elements. Be that as it may, unbalances in wind vitality are profoundly affecting the vitality transformation and this issue is regularly overwhelmed by utilizing a Doubly Fed Induction Generator (DFIG) [8].

II. MODELING OF DFIG

A fourth-order state space model is used for the modeling of the DFIG to address the synchronously pivoting coordinate framework (q-d-axis) as yielded (1)-(4) [1]

$$V_{qs} = r_s I_{qs} + \omega_e \lambda_{ds} + \frac{d}{dt}\lambda_{qs} \quad (1)$$

$$V_{ds} = r_s I_{ds} - \omega_e \lambda_{qs} + \frac{d}{dt}\lambda_{ds} \quad (2)$$

$$V_{qr} = r_r I_{qr} + (\omega_e - \omega_r)\lambda_{dr} + \frac{d}{dt}\lambda_{qr} \quad (3)$$

$$V_{dr} = r_r I_{dr} + (\omega_e - \omega_r)\lambda_{qr} + \frac{d}{dt}\lambda_{dr} \quad (4)$$

Where V_{qs} & V_{ds} are the q axis and d axis stator voltages. V_{qr}& V_{dr} are the q axis and d axis rotor voltages. I_{qs} &I_{ds}, are the q and d axis stator currents. I_{qr} & I_{dr} are the q and d axis rotor currents. λ_{qs} & λ_{ds} are the q and d axis stator fluxes. λ_{qr} & λ_{dr} are the q and d axis rotor fluxes. In the synchronously rotating reference frame, ω_r and ω_e represent the rotor and stator rotating angular velocity respectively. Again, r_s and r_r are the stator and rotor resistances. The equations for flux linkage are given by

$$\lambda_{qs} = L_s I_{qs} + L_m I_{qr} \quad (5)$$

$$\lambda_{ds} = L_s I_{ds} + L_m I_{dr} \quad (6)$$

$$\lambda_{qr} = L_m I_{qs} + L_r I_{qr} \quad (7)$$

$$\lambda_{dr} = L_m I_{ds} + L_r I_{dr} \quad (8)$$

Where L_r, L_s and L_m are the rotor, stator and mutual inductances, respectively, *with* $L_s = L_{ls} + L_m$ and $L_r = L_{lr} + L_m$. L_{ls} and L_{lr} are the self inductance of stator and rotor respectively.

The current equations can be obtained from equations (5) – (8):

$$I_{qs} = \frac{1}{\sigma L_s}\lambda_{qs} - \frac{L_m}{\sigma L_s L_r}\lambda_{qr} \quad (9)$$

$$I_{ds} = \frac{1}{\sigma L_s}\lambda_{ds} - \frac{L_m}{\sigma L_s L_r}\lambda_{dr} \quad (10)$$

$$I_{qr} = -\frac{L_m}{\sigma L_s L_r}\lambda_{qs} + \frac{1}{\sigma L_r}\lambda_{qr} \quad (11)$$

$$I_{dr} = -\frac{L_m}{\sigma L_s L_r}\lambda_{ds} + \frac{1}{\sigma L_r}\lambda_{dr} \quad (12)$$

Where leakage coefficient $\sigma = \frac{L_m L_r - L_m^2}{L_s L_r}$

A. *Dynamics of Doubly Fed Induction Generator*

State space structure of the dynamic system is critical. But to overcome this, diverse reproduction instruments like MATLAB is used. The basic state space structure assists with inquiring about the framework inside the transient condition. Reliable with the fundamental meaning, the co-ordinate axes are the 'n' variables (state) with time on the grounds that the verifiable variable is named the state space. The factors of the state space i.e. the state variables are included to work out the dynamic framework of conditions. Essentially these are the vitality putting away components contained inside the framework like inductor and capacitor. The essential state space equations are as per the following:

$$\begin{cases} \dot{X}(t) = AX(t) + BU(t) \\ Y(t) = CX(t) + DU(t) \end{cases} \quad (13)$$

Where X denotes the state vector. The output vector is denoted by Y. Again, A is state matrix, B is input matrix, C is output matrix, and D represent feed forward matrix. Also, equation (13) holds good for the system whose parameter does not vary with time.

$$\begin{cases} \dot{X}(t) = A(t)X(t) + B(t)U(t) \\ Y(t) = C(t)X(t) + D(t)U(t) \end{cases} \quad (14)$$

For the system whose parameters vary with time, Equation (14) is used. Also, matrices are depended on time. In the DFIG framework, the state factors are regularly flows or motions. In the accompanying area, the state space conditions for the DFIG in synchronously revolving outline has been determined with transition linkages as the state factors. The DFIG elements in the state space form can be obtained by substituting (9) - (12) into (1) - (4). It is given as:

$$\frac{d}{dt}\lambda_{qr} = -\frac{r_s}{\sigma L_s}\lambda_{qs} - \omega_e \lambda_{ds} + \frac{r_s L_m}{\sigma L_s L_r}\lambda_{qr} + v_{qs} \quad (15)$$

$$\frac{d}{dt}\lambda_{ds} = \omega_e \lambda_{qs} + \frac{r_s L_m}{\sigma L_s L_r}\lambda_{dr} - \frac{r_s}{\sigma L_s}\lambda_{ds} + v_{ds} \quad (16)$$

$$\frac{d}{dt}\lambda_{qr} = \frac{r_r L_m}{\sigma L_s L_r}\lambda_{qs} - (\omega_e - \omega_r)\lambda_{dr} - \frac{r_r}{\sigma L_r}\lambda_{qr} + v_{qs} \quad (17)$$

$$\frac{d}{dt}\lambda_{dr} = \frac{r_r L_m}{\sigma L_s L_r}\lambda_{ds} + (\omega_e - \omega_r)\lambda_{qr} - \frac{r_r}{\sigma L_r}\lambda_{dr} + v_{ds} \quad (18)$$

The matrix form of Equations (15) - (18) are as follows:

$$\begin{bmatrix} \dot{\lambda}_{qs} \\ \dot{\lambda}_{ds} \\ \dot{\lambda}_{qr} \\ \dot{\lambda}_{dr} \end{bmatrix} = \begin{bmatrix} -\frac{r_s}{\sigma L_s} & -\omega_e & \frac{r_s L_m}{\sigma L_s L_r} & 0 \\ \omega_e & -\frac{r_s}{\sigma L_s} & 0 & \frac{r_s L_m}{\sigma L_s L_r} \\ \frac{r_r L_m}{\sigma L_s L_r} & 0 & \frac{r_r}{\sigma L_r} & (\omega_e - \omega_e) \\ 0 & \frac{r_r L_m}{\sigma L_s L_r} & (\omega_e - \omega_e) & -\frac{r_r}{\sigma L_r} \end{bmatrix} \begin{bmatrix} \lambda_{qs} \\ \lambda_{ds} \\ \lambda_{qr} \\ \lambda_{dr} \end{bmatrix} + \begin{bmatrix} 1 & 0 & 0 & 0 \\ 0 & 1 & 0 & 0 \\ 0 & 0 & 1 & 0 \\ 0 & 0 & 0 & 1 \end{bmatrix} \begin{bmatrix} v_{qs} \\ v_{ds} \\ v_{qr} \\ v_{dr} \end{bmatrix}$$

III. POWER CONVERTERS

Vector control method with application to DFIG machine is very attracting for the generating and variable speed drive applications. In variable speed drive application, the alleged slip power recuperation plan might be a typical practice here the office because of the rotor slip underneath or above synchronous speed is recouped to or provided from the office source prompting a profoundly productive variable speed framework. By utilizing well-known Static Scherbius drive for bi directional force stream, slip power control are regularly achieved.

Retrieval Number: 100.1/ijitee.I92880710921
DOI: 10.35940/ijitee.I9288.0710921
Journal Website: www.ijitee.org

Published By:
Blue Eyes Intelligence Engineering and Sciences Publication

The primary bit of leeway for the DFIG is that the office hardware utilized consecutive converter that handles a small amount of all out framework power. The back to back converter comprises of two converters for example Generator Side Converter (GSC) and Rotor Side Converter (RSC). These convertors are connected through a dc link capacitor for vitality stockpiling reason.

The power converter is shaped from a consecutive converter interfacing the rotor circuit and subsequently the network as appeared in Fig 1. The converters are ordinarily produced by IGBTs based freewheeling diodes of voltage source inverters (see Fig 1), which empower a bi-directional force stream. A RL channel is given on the GSC side to attenuate the switching harmonics provided to the grid.

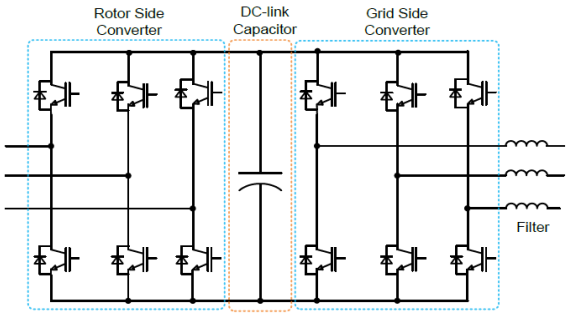

Fig.1. Bidirectional power converter with DC link

A. Rotor Side Converter

The RSC is constrained by two factors by using its power rating. These are reactive power limit and explicit maximum slip power. The rotor side converter can be treated as a voltage source converter of current controlled type. The stator side dynamic power, rotor speed and the reactive power control is the main focus of RSC.

B. Grid Side Converter

To restrain the setbacks in the converter, the power rating of the GSC is regularly works at an unity power factor [2]. To achieve this it is mainly operated with slip power. The DC link voltage of convertor is normally controlled through GSC. The converter can in like manner be utilized to help grid reactive power during an inadequacy [3]. To update the framework power quality, the grid side converter is also be used in this purpose [4].

The measure of energy put away in the dc-link capacitor can be composed as:

$$E_c = \int P\,dt = \frac{1}{2}CV_{DC}^2 \qquad (20)$$

Where P indicates the total power stream into the capacitor, V_{DC} is the voltage of the capacitor and C is the DC-link capacitor worth. P = Pr - Pg, where Pg is the grid power outflow and Pr is the rotor power inflow.

IV. PITCH CONTROLLER AND ESTIMATION OF C_P

The turbine is the prime mover of wind energy conversion system that empowers the transformation of kinetic energy of wind E_w into mechanical power Pm and at last into electricity [5]

$$\begin{cases} P_m = \frac{\partial E_W}{\partial t} C_p = \frac{1}{2}\rho A V_w^2 C_p \\ C_p(\lambda,\beta) = 0.5176\left(\frac{116}{\lambda_i} - 0.4\beta - 5\right)e^{-21/\lambda_i} + 0.0068\lambda \end{cases} \qquad (21)$$

Where V_w is the wind velocity at the focal point of the rotor (m/sec), ρ is air density (kg/m^3), $A = \prod R^2$ is the frontal area of the wind turbine (m^2) and R is the rotor radius. C_p is the performance coefficient which thus relies on the turbine qualities (β - blade pitch angle and λ - tip speed proportion) that is responsible for the losses in the energy transformation process. The numerical estimation of C_p utilized right now is taken from and $\lambda_i = f(\lambda,\beta)$ is given by

$$\begin{cases} \lambda = \omega_t R \\ \frac{1}{\lambda_i} = \frac{1}{\lambda + 0.08\beta} - \frac{0.035}{\beta^3 + 1} \end{cases} \qquad (22)$$

Where R is the wind turbine blade radius and ω_t is the turbine speed. Since$C_p = f(\lambda,\beta)$, the plot of Cp versus λ at different estimations of β is appeared in Figure 2. At the point when the wind speed increments past the rated value, the electromagnetic torque isn't adequate to control rotor speed since this prompts an over-burden on the generator and the converter. To forestall rotor speed from getting excessively high, the extricated power from approaching wind must be constrained. This should be possible by decreasing the coefficient of execution of the turbine (the Cp value). As clarified before, the Cp value can be controlled by changing the pitch angle (see Figure 2). Modifying the pitch angle β implies somewhat rotating the turbine blades along the axis. The blades significantly substantial in a huge turbine. Therefore, the rotation must be encouraged by either hydraulic or electric drives. The pitch controller model is shown in Figure 3. The lower part of the pitch controller demonstrated in the Figure 3 is the turbine speed regulator, while the upper part represents an aerodynamic power limiter. The whole control can be carried out by means of PI controllers.

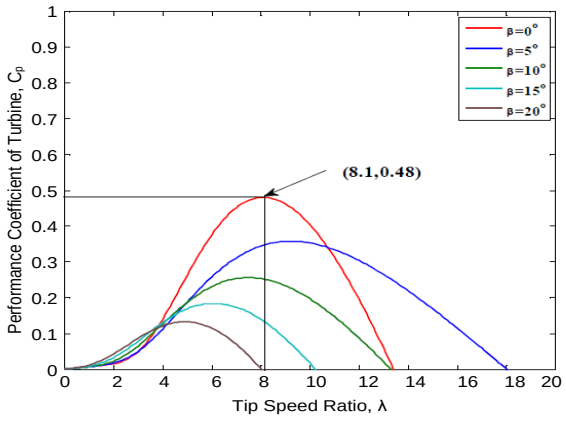

Fig. 2. **C_P – λ characteristic curves**

Published By:
Blue Eyes Intelligence Engineering
and Sciences Publication

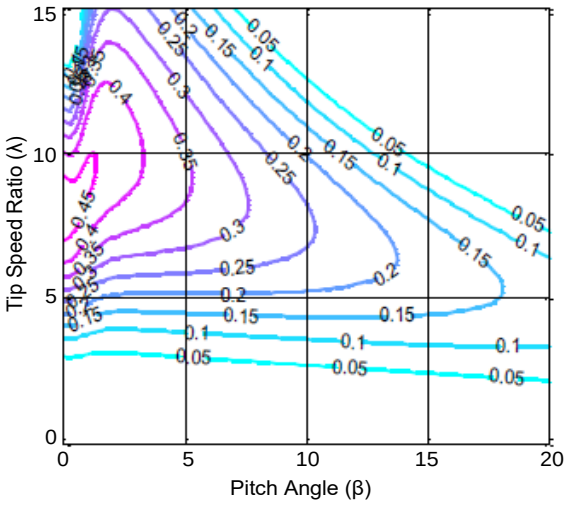

Fig.3. Performance Coefficient, C_p Contour

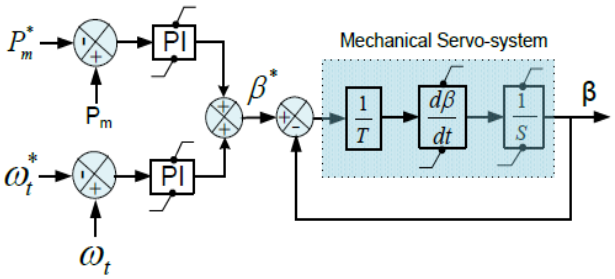

Fig.4. Pitch angle control scheme using PI controllers

V. CONTROL OF DFIG USING WECS

The two segments of a DFIG-based control framework are mechanical control of turbine speed through blade pitch angle and electrical control of the DFIG. Control of the DFIG is achieved by incorporating control of the RSC and GSC through the variable frequency converter. Again for decoupled control of active and reactive power in a DFIG based wind turbine the RSC is used. This encourages high adaptability which empowers the turbine to catch most extreme energy from wind and simultaneously to give reactive power backing to the grid. The purpose of the GSC is to keep the link voltage steady paying little heed to the size and bearing of the rotor power.

A. Dynamics of RSC control structure

The RSC control structure mainly comprises of two vector control structures. One is internal current control loop and the other one is outer control loop. The d and q axes rotor currents, i.e. I_{dr} and I_{qr} are autonomously controlled in previous one. While the active and reactive power of the stator is coordinated for latter one. The stator voltage direction (SVO) control working standard for a DFIG is depicted in [6]. Where the q-axis of the turning reference outline is adjusted to the stator voltage i.e. $V_{ds} = 0$ and $V_{qs} = V_s$. The stator side flux can also be controlled by the use of PI controller. The RSC vector control method is shown in Fig. 4.

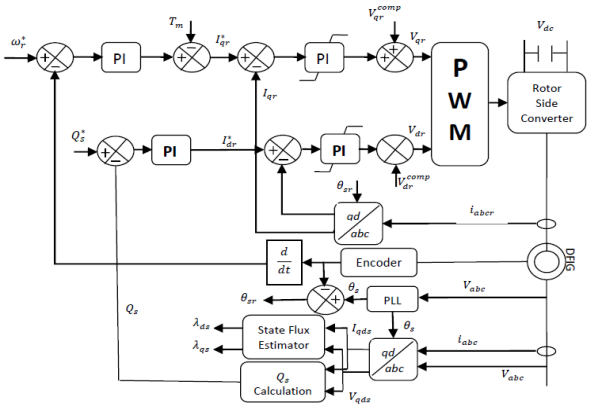

Fig.5. Block diagram of RSC control system

The dynamics of the system are obtained as:

$$\frac{I_{qr}}{I_{qr}^*} = \frac{pk_{qp}+k_{qi}}{p^2\sigma L_r+p(r_r+k_{qp})+k_i} = \frac{\frac{1}{\sigma L_r}(pk_{qp}+k_{qi})}{p^2+p\frac{1}{\sigma L_r}(r_r+k_{qp})+\frac{1}{\sigma L_r}k_{qi}} \quad (23)$$

$$\frac{I_{dr}}{I_{dr}^*} = \frac{pk_{dp}+k_{di}}{p^2\sigma L_r+p(r_r+k_{dp})+k_{di}} = \frac{\frac{1}{\sigma L_r}(pk_{dp}+k_{di})}{p^2+p\frac{1}{\sigma L_r}(r_r+k_{dp})+\frac{1}{\sigma L_r}k_{di}} \quad (24)$$

Supposing the suitable parameters of controller is critical to increase great execution despite the fact that the whole structure may have the option to work for a wide scope of parameters. Numerous analysts select the additions dependent on the experience or just by experimentation. This isn't acceptable particularly when the control framework is intended for another framework. The most significant target is to keep up the framework steadiness by choosing proper control parameters. And afterward those parameters can be adjusted comparing to the predefined execution prerequisite. There are a few techniques that can be utilized to decide the framework parameters that can keep the entire framework in the steady region.

One of the techniques, optimization of the closed-loop Eigen value locations is done by utilizing Butterworth polynomial [7]. The Eigen values obtained through the Butterworth technique consistently finds on a circle with radius ω_0 in the left-half s-plane, along with center at the origin.

The second order Butterworth polynomial for the transfer function is given as:

$$p^2 + \sqrt{2}\omega_0 p + \omega_0^2 = 0 \quad (25)$$

Also, from the Fig. 4, we get

$$V_{dr}^* = \left(k_{dp} + \frac{k_{di}}{p}\right)(I_{dr}^* - I_{dr}) \quad (26)$$

The parameters of PI controller are dictated by contrasting the coefficients in (25) with the denominator polynomials of the relating dynamic models and afterward picking suitable ω_0 .

$$k_{qp} = k_{dp} = \sqrt{2}\omega_0\sigma L_r - r_r \quad (27)$$

Retrieval Number: 100.1/ijitee.I92880710921
DOI: 10.35940/ijitee.I9288.0710921
Journal Website: www.ijitee.org

Published By:
Blue Eyes Intelligence Engineering and Sciences Publication

$$k_{qi} = k_{di} = \sigma L_r \omega_0^2 \quad (28)$$

Where ω_0 is the current controller bandwidth, which relies on the design value.

$$T_m = k_{opt} V_w^2 \quad (29)$$

Similarly, contrasting denominator of (29) with second order Butterworth polynomial,
i.e. $p^2 + \sqrt{2}\omega_{0wr} p + \omega_{0wr}^2$, The gains of the PI controller are obtained as

$$k_{Pwr} = \sqrt{2}\omega_{0wr} \frac{2J}{P} \quad (30)$$

$$k_{Iwr} = \omega_{0wr}^2 \frac{2J}{P} \quad (31)$$

Again,

$$\frac{Q_s}{Q_s^*} = \frac{\frac{1}{\nabla}(pP_{PQS} + k_{IQS})}{p^2 + p\frac{k_{PQS}}{\nabla} + \frac{k_{IQS}}{\nabla}} \quad (32)$$

Similarly second order Butterworth polynomial can be contrasted with the denominator of (32) with,
i.e., $p^2 + \sqrt{2}\omega_{QS} p + \omega_{QS}^2$ the gains of the PI controller are obtained as

$$k_{PQS} = \sqrt{2}\omega_{0QS}\Delta \quad (33)$$

$$k_{IQS} = \omega_{QS}^2 \Delta \quad (34)$$

VI. DYNAMICS OF GSC CONTROL STRUCTURE

The general vector control structure of the GSC is shown in Fig. 5. Here by controlling current in synchronous reference frame, control of DC-link voltage V_{dc} and reactive power trade among GSC and power grid is cultivated [8].

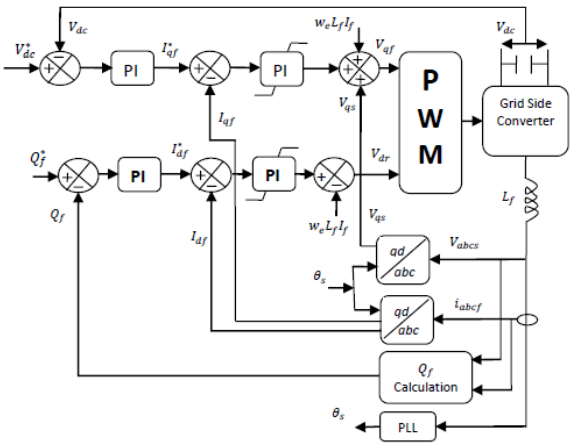

Fig.6. Block diagram of GSC control system

Now, the dynamics of the system in DC-link is given by:

$$\frac{V_{dc}}{V_{dc}^*} = \frac{\frac{1}{C_{dc}}(pk_{Pdc} + k_{Idc})}{P^2 + p\frac{k_{Pdc}}{C_{dc}} + \frac{k_{Idc}}{C_{dc}}} \quad (35)$$

By comparing denominator of (35) with second order Butterworth order polynomial, i.e., $p^2 + \sqrt{2}\omega_{0dc} p + \omega_{0dc}^2$, The gains of the PI controller are obtained as

$$k_{Pdc} = \sqrt{2}\omega_{0dc} C_{dc} \quad (36)$$

$$k_{Idc} = C_{dc}\omega_{0dc}^2 \quad (37)$$

Where ω_{0dc} is the DC-voltage controller bandwidth.
For, inner current control

$$\frac{I_{qf}}{I_{qf}^*} = \frac{\frac{1}{L_f}(pk_{P1} + k_{I1})}{P^2 + p\frac{1}{L_f}(r_f + k_{P1}) + \frac{1}{L_f}k_{I1}} \quad (38)$$

Comparing denominator of (38) with second order Butterworth second order polynomial gives:

$$k_{P1} = \sqrt{2}\omega_{0c} L_f - r_f \quad (39)$$

$$k_{I1} = L_f \omega_{0c}^2 \quad (40)$$

Where ω_0 is the current controller bandwidth.

VII. PHASE LOCKED LOOP

A Phase Locked Loop (PLL) is intended to characterize the reference angle for q-d change with the goal that the stator voltage can be adjusted along the q-axis and is included in the general model of the framework to construct the planned framework more practical.

$$\frac{\theta_s}{\theta_i} = \frac{pV_s k_{P\_pu} + V_s k_{I\_pu}}{p^2 + pV_s k_{P\_pu} + V_s k_{I\_pu}} \quad (41)$$

Now comparing denominator of (41) with second order Butterworth second order polynomial $p^2 + \sqrt{2}\omega_{0\_pu} p + \omega_{0\_pu}^2$, the parameters of the controller are

$$k_{I\_pu} = \omega_{0\_pu}^2 / V_s \quad (42)$$

Where ω_{0_pu} is the PLL controller bandwidth.

VIII. SIMULATION RESULTS

Table.1 and Table.2 give the parameters of machines and PI controllers utilized for the simulation results implementing above methodology. In this paper, the bandwidth of external current controller is supposed as one tenth of the bandwidth of internal current controller and the switching frequency is 1 kHz.

$\omega_{sw} = 2\pi f_{sw} = 6280\ rad/sec$
And $\omega_{inner} = \frac{\omega_{sw}}{10}$; $\omega_{outer} = \frac{\omega_{inner}}{10}$

$$\omega_{inner} = \omega_0 = \omega_{0c} = 628\ rad/sec$$

$\omega_{outer} = \omega_{odc} = \omega_{oQs} = \omega_{oQf} = 62.8\ rad/sec$ and
$\omega_{owr} = 0.628\ rad/sec$

Table.1 Parameters of the machine

V_s	562.49 V	L_f	1.98 mH
N	1	r_f	2 mΩ
P	4	r_s	2.28 mΩ
σ	0.045	r_r	2 mΩ
J	17.98	C_{dc}	60 mF
L_m	2.68 mH		
L_r	2.98 mH		
L_s	2.87 mH		

Table.2 Parameters of PI controllers

K_{qp}	1.72	K_{qi}	684.9
K_{dp}	1.73	K_{di}	684.5
K_{Pdc}	6.52	K_{Idc}	310.24
K_{Pwr}	8.34	K_{Iwr}	3.45
K_{PQs}	0.00023	K_{IQs}	0.0012
K_{PI}	1.67	K_{II}	758.94
$K_{P\lambda s}$	75.24	$K_{I\lambda s}$	3817.4
K_{P_pll}	2.21	K_{I_pll}	1268.39
K_{PQf}	0.00019	K_{IQf}	0.00089

Fig.7 shows grid current is synchronized and for better deceivability the time offset is adjusted to 0.7 sec. So the control methodology is sensible the application to grid side converter based wind energy conversion system.

Fig. 8 shows the plot for reference angle from PLL to adjustment of the stator voltage along the q-axis.

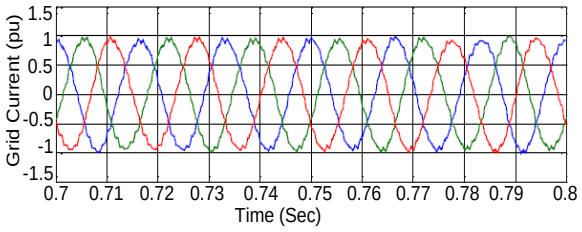

Fig. 7 Grid Current

Furthermore, simulation studies are done for a 2.5 MW DFIG-based WECS to confirm the viability of above depicted control framework under differing wind speed. Two distinctive simulation studies are accomplished for evaluating the performance of the control system talked about above. In the first case appeared in Figures 8 and 9, the progression decline in wind speed from 12 m/s to 8 m/s is made at t = 4 s, the rotor speed and active power output yield fluctuates as per wind speed where as reactive power is directed to a steady value. Again at t = 4 s, step increment in reactive power supplied by stator side is applied and at t = 6 s, step increment in reactive power supplied by GSC is applied. The two cases don't influence the active power output of the DFIG which demonstrates the decouple control of active and reactive power.

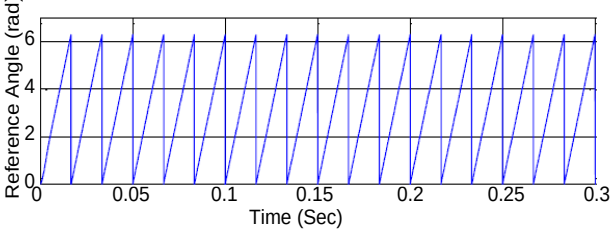

Fig. 8. Reference angle from PLL

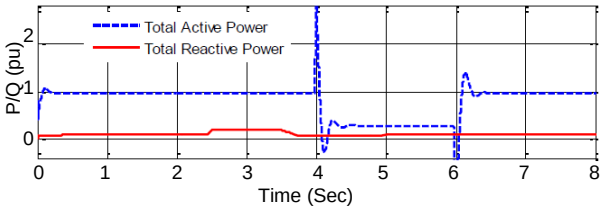

Fig. 9. Total Active and Reactive Power

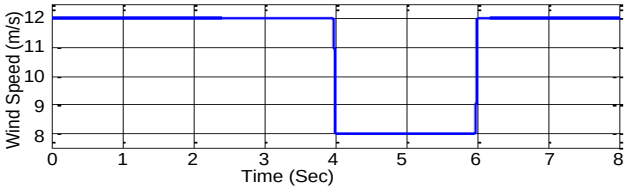

Fig. 10 Step Change in Wind Speed

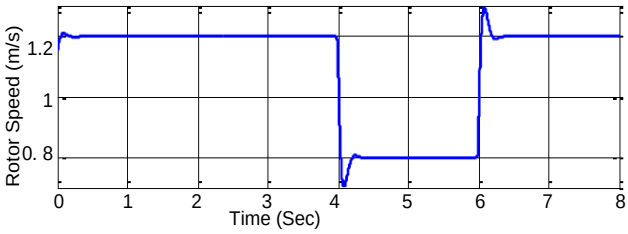

Fig. 11 Step Change in Rotor Speed

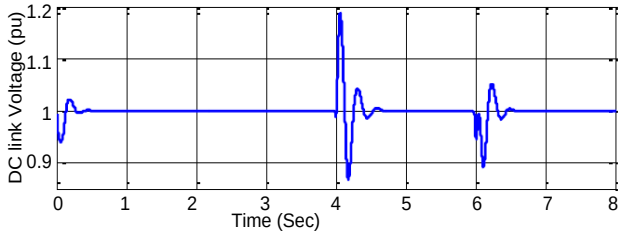

Fig. 12 Step Change in DC link Voltage

The progression change in rotor speed and direct current link voltage are appeared in Fig. 10 and Fig. 11 respectively.

IX. CONCLUSION

In this paper, modeling and controller development for variable-speed variable-pitch wind turbine is exhibited. Vector control method is actualized for decoupled control of reactive power and active power connected to power grid. The decoupled control of the rotor speed, stator side supplied reactive power, DC-link voltage and GSC supplied reactive power is confirmed by computing the overall dynamic model of the framework. The dynamic characteristics of the doubly fed induction generator based wind energy conversion systems are contemplated during changing wind speed input to the wind turbine.

REFERENCES

1. Krause, O. Wasynczuk, and S. D. Sudhoff, "Analysis of Electric Machinery and Drive Systems", IEEE Press, Wiley-Interscience, John Wiley & Sons, Inc., New Jersey, 2002.

Retrieval Number: 100.1/ijitee.I92880710921
DOI: 10.35940/ijitee.I9288.0710921
Journal Website: www.ijitee.org

Published By:
Blue Eyes Intelligence Engineering and Sciences Publication

2. Wei Qiao, Wei Zhou, J.M. Aller, and R.G. Harley, “Wind Speed Estimation Based Sensor less Output Maximization Control for a Wind Turbine Driving a DFIG,” IEEE Trans. on Power Electronics, vol. 23, no. 3, pp. 1156-1169, May 2008.
3. Hansen, and G. Michelle, “Voltage grid support of DFIG wind turbines during grid faults," in Proc. European Wind Energy Conference and Exhibition, May 2007.
4. E. Tremblay, A. Chandra, and P. Lagace, “Grid-side converter control of DFIG wind turbines to enhance power quality of distribution network," in Proc. IEEE Power Engineering Society General Meeting, Jun. 2006.
5. Endusa Billy Muhando, Tomonobu Senjyu, Aki Uehara, Toshihisa Funabashi, and Chul-Hwan Kim, “LQG Design for Megawatt-Class WECS With DFIG Based on Functional Models' Fidelity Prerequisites,” IEEE Trans. on Energy Conversion, vol. 24, no. 4, pp. 893-904, Dec. 2009
6. Bakari Mwinyiwiwa, Yongzheng Zhang, Baike Shen, and Boon-Teck Ooi, “Rotor Position Phase-Locked Loop for Decoupled P-Q Control of DFIG for Wind Power Generation,” IEEE Transactions on Energy Conversion, vol. 24, no. 3, pp. 758-765, Sept. 2009.
7. Gan Dong, “Sensor less and Efficiency Optimized Induction Machine Control with Associated Converter PWM Modulation Schemes," Ph.D. dissertation, Tennessee Technological University, Dec. 2005.
8. Krause, O. Wasynczuk, and S. D. Sudhoff, Analysis of Electric Machinery and Drive Systems, IEEE Press, Wiley-Interscience, John Wiley & Sons, Inc., New Jersey, 2002.

AUTHORS PROFILE

Syed Sarfaraz Nawaz, pursuing PhD from JNTUH. He had done his M.Tech with DISTINCTION in 2010 from GRIET Hyderabad and his B.Tech FIRST CLASS in 2007 from SSITS affiliated to JNTUH. He had overall experience of 12 years. He is familiar with software’s like MATLAB, LABVIEW, EAGLE, KEIL, E-Tap Software, Proteus, Multisim, VISIM, PSIM etc and worked on DSPACE1104,F28086/7 DSP Control boards, PCI6221 Control Card and TI control boards. His areas of interest are Power Electronics, Power Systems, and Machines.

Tara K. Sandipamu, completed her Ph. D in FACTS, from JNTU Hyderabad in 2008. Her areas of interests are Power Electronics, Control Systems, Fundamentals of Electrical Engineering, Energy Systems and Power Systems. She worked as Assistant Director, Academic Staff College, University Grants Commission, JNTUH. As she had strong work experience, she also served as Deputy Director, Academic Staff College. Now she is Controller of Examinations.